University of Genoa

Master's Program in Bioengineering

Thesis submitted in partial fulfillment of the requirements for the title of Master of Bioengineering

An innovative methodology combining TMS, EMG and fNIRS to explore the dynamics of interhemispheric inhibition

Elena Monteleone

Marzo 2024

Thesis advisor: Prof.ssa Laura Bonzano
Thesis co-advisor: Prof. Marco Bove
Thesis co-advisor: Dr.ssa Costanza Iester

Contents

Summary

The aim of this work was to evaluate the cortical correlates of the ipsilateral silent period (iSP). To achieve this aim, the Transcranial Magnetic Stimulation (TMS) was used to stimulate the left hemisphere, the functional Near InfraRed Spectroscopy (fNIRS) to record cortical activation of the right hemisphere and the electromyography (EMG) to acquire the muscle activation. The experiment involved a total of 15 subjects, who were asked to perform a maximal isometric contraction of the first dorsal interosseous (FDI) muscle of the thumb with the left hand or with both hands. From the EMG data, the iSP area was performed, while, from the fNIRS data, the hemodynamic functional responses of the twenty Brodmann areas was calculated. Confirming the literature, EMG results showed a higher iSP area when both hands were contracted. fNIRS results showed different active areas during a maximal isometric contraction which involves not only the motor cortex but also parietal areas. The presence of iSP reduced BAs activation. The correlation between EMG and fNIRS results showed a higher inhibition with a higher BA4 activity. Interestingly, these results could be justified by considering the resulting BA4 activation as the combination of different neuronal population (i.e., pyramidal neuron and inter-inhibitory neurons). Moreover, the iSP area

was explained by parietal areas when only the left hand was contracted, while by motor and parietal areas when both hands were contracted. In general, the contribution of parietal area to iSP area could be explained by a feedback mechanism, while the BA4 contribution by a forward mechanism. To conclude, these finding pave the way for numerous avenues of future research and serve as a prime foundation for unraveling the dynamics of the ipsilateral silent period, a phenomenon that remains largely unexplored.

Chapter 1

Introduction

During everyday life, several actions requiring the coordination of limbs take place. The ability to precisely perform coordinated movements, both unimanual and bimanual tasks, requires interhemispheric interaction. The corpus callosum is a bundle of nerve fibres that connect the left and the right hemispheres. Thanks to the corpus callosum, it is possible to facilitate the comunication between the two hemispheres, allowing them to work together in various cognitive and motor functions. Moreover, the corpus callosum plays a crucial role in integrating information and coordinating activities between the two halves of the brain. The interhemispheric interaction could be measured by two indexes: the contralateral silent period (cSP) and the ipsilateral silent period (iSP). Even though cSP and iSP share similar features, they may reflect slightly different components. cSP is investigated as a possible surrogate of corticospinal inhibition, most likely mediated by gamma-aminobutyric acid (GABA) B receptors within M1. Conversely, iSP is thought to reflect transcallosal inhibition and thus be entirely of cortical

origin(REF:[Rebello-Sanchez *et al.*, 2022]). To obtain both the cSP and iSP values, the simultaneous use of transcranial magnetic stimulation (TMS) and electromyography (EMG) is required.

In this research, we will focus on iSP. What is missing in literature is the exploration of the silent periond neural correlates to investigate the nature of the signal. This could also involve non-motor areas such as the prefrontal or parietal regions. Therefore, the goal of this thesis work is to evaluate the correlation between the iSP relating to the left hemisphere and the activation of different areas in the right hemisphere. To achieve this aim the combination of three brain investigation methods (TMS, EMG and functional Near InfraRed Spectroscopy(fNIRS)) was required.

1.1 Trascranical magnetic stimulation

TMS was introduced in 1985 as a noninvasive method for stimulating the human brain. It was demonstrated that a single TMS pulse to the primary motor cortex could elicit responses in the muscles that received corticospinal input from the stimulated cortical region. Since this time, multiple TMS approaches including single pulse, paired pulse and repetitive TMS (rTMS) have been adopted and applied to a wide variety of tasks and patient populations[Hupfeld *et al.*, 2020]. In general, single-pulse TMS (including paired-pulse TMS) is used to explore brain functioning, whereas rTMS is used to induce changes in brain activity that can last beyond the stimulation period [Klomjai *et al.*, 2015].

TMS induces currents in the brain via Faraday's principle of electromag-

netic induction. As the magnetic field changes rapidly, circular electrical currents are induced [Tofts, 1990]. The currents flow in a plane perpendicular to the magnetic field. Consequently, the induced currents by TMS circulate in a ring-shaped region beneath the coil. If the coil is placed flat on the scalp, currents flow in a plane parallel to both the coil and the scalp. The force of magnetic field induced by TMS can be reduced by extracerebral tissues (scalp, bone, meninges), but it is still able to induce an electrical field sufficient to depolarize superficial axons and to activate networks in the cortex. However, because the impedance of gray matter is greater than that of white matter, electrical currents in subcortical structures are weaker than in superficial layers, so subcortical structures such as the basal ganglia and thalamus are not activated by TMS. TMS preferentially activates neurons oriented horizontally in a plane parallel to both the coil and the brain surface. TMS applied to the motor cortex induces descending bursts in the pyramidal tract which induce glutamate release in cortico-motoneural synapses. Provided that the discharges are strong enough to exceed the activation threshold, an action potential is subsequently triggered in spinal motor neurons. These action potentials propagate along peripheral motor axons to induce a muscle response. The resulting muscle responses can be recorded as motor evoked potentials (MEPs), which are spikes in muscle activity due to activation of corticospinal neurons. The MEP is recorded on the EMG using surface electrodes applied to the muscle belly.

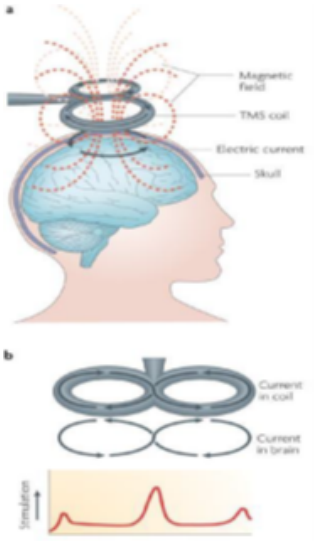

Figure 1.1: a) TMS positioned on the scalp to stimulate. b)TMS coil and MEP.

In practice, the peak-to-peak amplitude of the MEP and the motor threshold (MT), defined by the minimum TMS intensity required to evoke a MEP of at least 50 mV in approximately 50 of 5–10 consecutive trials, are both parameters used to estimate the 50% excitability of the corticospinal pathways. However, they rely on different physiological mechanisms. The MT, which depends on excitability of cortico-cortical axons and their excitatory contacts to corticospinal neurons, is influenced by agents blocking voltage gated sodium channels that are crucial in regulating axon excitability and by agents acting on ionotropic non-Nmethyl-D-aspartate (non-NMDA) glutamate receptors such as ketamine that are responsible for fast excitatory synaptic transmission in the cortex. In contrast, other neurotransmitters and neuromodulator systems such as GABA, dopamine, norepinephrine, serotonin or

acetylcholine have no effect on MT. As for MT, the MEP can be depressed by agents that inactivate sodium channels such as volatile anesthetics. MEP reduction is hypothesized to result from reduced excitability of I-waves due to sodium-channel inactivation, which leads to decreased action potential firing and in turn reduces calcium entry at the presynaptic terminal and finally synaptic transmission. Moreover, MEP amplitude was found to vary after the application of modulators of inhibitory and excitatory transmission in neuronal networks. For instance, MEP is depressed by modulators of GABAA receptors or increased by dopamine agonists and various norepinephrine agonists. Of note, changes in MEP amplitude can occur without significant changes in MT, which supports the notion of a fundamental difference in physiology between the two measures.

The path and intensity of an electric field produced within the brain via TMS are influenced by numerous physical and biological factors. These encompass the waveform of the magnetic pulse; the shape and orientation of the coil; the strength, frequency, and configuration of the stimulation; the orientation of induced current pathways within the brain; and the presence of excitable neural components. Different coil shapes, such as the circular coil, figure-of-eight coil, double-cone coil, air-cooled coil, Hesed coil, c-Core coil, and circular crown coil, have been developed. Circular coils widely distribute currents, activating superficial cortical layers and are recommended for large and superficial motor areas like upper-limb motor areas. In contrast, the figure-of-eight coil provides focused stimulation, concentrating the electric field under its center for a more precisely defined area. The double-cone coil, with its ability to reach deep cortical layers, is suitable for stimulating motor

areas of lower limbs within the interhemispheric fissure. However, it lacks focus, as a single TMS via a double-cone coil over M1 can elicit bilateral responses in upper and lower limbs, along with facial muscle contractions. The direction of current lines is influenced by the coil's orientation and position over brain gyri and sulci. Compared to single-pulse TMS, paired-pulse TMS consists of two successive pulses through the same coil, delivered with a short inter-stimulus interval (ISI) of a few milliseconds or a long ISI (from tens to hundreds of milliseconds). In practice, both pulses are applied over the same point of the dominant hemisphere over the motor cortex. This method is used to explore inhibitory or excitatory intracortical networks depending on the intensity and ISI used. Nevertheless, paired-pulse TMS can reveal inhibitory cortical networks more easily than excitatory networks, which are less investigated. Two TMS pulses can also be delivered over each hemisphere at the same point of the motor cortex to explore inter-hemispheric inhibition (or transcallosal inhibition). Contrary to single-pulse TMS, rTMS can change and modulate cortical activity beyond the stimulation period, as a potential method for the treatment of neurological and psychiatric disorders.

The physiological foundations of the after-effects following rTMS remain unclear. Numerous arguments suggest that the mechanisms underlying these after-effects share similarities with long-term potentiation (LTP) and long-term depression (LTD) observed in animals. LTP and LTD refer to enduring alterations in synaptic strength that can occur under experimental conditions following brief high-frequency stimulation. LTP is characterized by an increase in synaptic strength, while LTD signifies a decrease. [Klomjai *et al.*, 2015]

1.2 Electromyography

The EMG is a diagnostic technique used to evaluate the electrical activity of muscles. It involves the insertion of surface or needle electrodes into the muscle of interest to record and analyze the electrical signals produced during its functioning.

Two approaches may be identified based on the receiving sensor typology: intramuscular (imEMG) and superficial electromyography (sEMG). sEMG allows recording of entire muscular biopotential signals from several muscle groups, evaluating the functional condition of a muscular area rather than simply a single motor unit. The surface approach uses the characteristic of large-scale electrical conductivity, which eliminates the influence of electrode proximity from the signal source on its form and character. This approach enables the use of non-invasive electrodes, removing the pain and risk of monitoring. Surface electromyography detects and monitors the biopotentials generated when a neurological or electrochemical stimulus triggers muscle fibers. The responses include data on muscle activation, tone, and exhaustion, as well as recruitment and synchronization patterns. sEMG signals are nondeterministic, noisy, and complex; they also have small amplitudes and a frequency range. As a result, their acquisition is complicated. Noise from the electronic acquisition equipment, skin-electrode interface, and power lines all contribute to background noise. Therefore, a well-designed system is needed to enhance the acquisition and analysis of EMG signals. Such acquisition systems comprise electrodes, pre-processing stages (preamplifiers and filters), amplifiers, analog-to-digital conversions, power supply sections, and wireless transmission modules. [Al-Ayyad *et al.*, 2023]

ImEMG provide an alternative source of EMG signals and address some of the difficulties associated with sEMG-based control, such as maintaining robust electrode contact with the skin; it also provides addition benefits, such as the ability to record from deep muscles with little EMG crosstalk. However, ImEMG has been clinically infeasible, as it requires the use of percutaneous wire/needle electrodes to transmit signals to the prosthesis. [Smith and Hargrove, 2013] Given his invasiveness, sEMG will be used in this study.

Since the EMG output signal is noisy, it is necessary to use some algorithms to reduce the noise, such as, digital filters, averaging, and smoothing. This task is accomplished through a combination of analog hardware and digital signal processing techniques. By amplifying the neurophysiological signal voltage and minimizing the background noise, an optimal 'signal to noise ratio' was achieved. To attenuate the unwanted noise, it's used a differential amplifier that magnifies the signal. The amplified signal is measured using an analogue-to-digital convertor (ADC) and the voltage values stored as an array of numbers. An EMG machine also offers stimulation devices to excite nerves and muscles. These may generate electrical, visual or auditory stimuli. External devices providing other forms of stimulation, e.g. magnetic field, contact heat, reflex hammer, etc. can be interfaced to provide timing signals through so-called 'triggers'. To achieve this, some instruments pass the digitized signals through a 'digital-to-analogue convertor (DAC)', to convert digital signals (with much less noise) into analogue form. The EMG machine displays signals, measurements, and the settings of the amplifier and stimulator. The latter can be changed using a dedicated control panel or us-

ing software commands via a mouse or computer keyboard. The software is responsible for signal processing and for generating reports. Databases can be created, and remote review used for second opinions or to help with interpretation.

1.2.1 EMG-Amplifier

The amplifier stands out as a crucial element in determining the quality of the electrodiagnostic system. Achieving selective amplification of neurophysiological potential while suppressing background noise is made possible using a 'differential' amplifier (DA), which requires inputs from three electrodes. Historically, these electrodes were denoted as 'G1', 'G2', and 'ground', with G1 and G2 referring to the vacuum tube grids in outdated amplifiers. Later, these inputs were renamed as 'active', 'reference', and 'ground'. In electrodiagnostic recording, 'ground' refers to a reference point on the amplifier circuit for voltage measurement. Beyond electrodiagnostics, 'ground' also refers to a connection in power supply and wall outlets. The 'reference' electrode is presumed to be electrically silent but does record large volume-conducted potentials, such as the electrocardiogram (ECG).

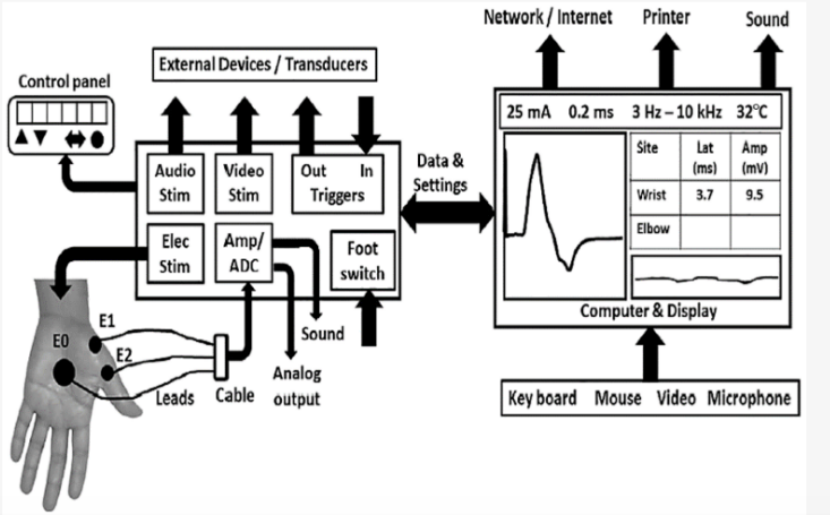

Figure 1.2: Example EMG.

The recommended terms for the three connections to the amplifier are 'E1', 'E2', and 'E0'. In most systems, these inputs are color-coded as black (E1), red (E2), and green (E0). The amplifier doesn't amplify the voltage at E1 or E2 inputs individually; rather, it magnifies their difference, earning it the name 'differential amplifier' due to its 'differential' gain. This differential gain allows the elimination of ambient noise, particularly the substantial ECG potential, enabling the selective amplification of the small neurophysiologic signal within high-amplitude noise. The 'common signal' at E1 and E2 inputs is also amplified, but much less. The ratio of output to input noise voltage, produces a 'common mode gain' for the amplifier. A DA should have a high differential gain and low common mode gain. These properties are defined in a single characteristic called the common mode rejection ratio (CMRR). It is reported in units of decibels and calculated as:

$$CMRR(dB) = 20 \log \frac{Differential\ gain}{Common\ mode\ gain} \tag{1.1}$$

Electronic components of the amplifier contribute some noise, addressed by connecting E1, E2, and E0 electrodes and measuring the amplifier output. The signal's peak-peak amplitude or root mean square (RMS) value is reported, typically less than 1 μ but also depends on the amplifier range and the filter settings. High amplifier range (i.e. low gain setting) and short band width will give lower noise. The amplifier is also characterized by its 'input impedance'. As the amplifier needs a tiny amount of current to measure a voltage, the input impedance needs to be several orders of magnitude larger than the input impedance of the generator of the voltage, i.e. muscle, nerve, body fluids. Low impedance makes the system more sensitive to environmental noise. It may also underestimate signal amplitude. Modern systems introduce 'switching amplifiers,' allowing users to select inputs via software, facilitating multiple channels for recordings, often employed in evoked potential studies.. These channels usually have a much lower CMRR. Such channels may not be suitable for recording signals with high frequencies (e.g., needle EMG) or when the electrodes differ in their impedances (surface versus needle). In clinical practice, a mix of signals and 'noise' is obtained, where the 'noise' encompasses irrelevant information for diagnostic purposes. Filtering, limited to attenuating specific frequency components in the signal, is employed to address undesired signal components. EMG equipment inte-

grates digital computers for data sampling, storage, and signal processing. After amplification, the analog-to-digital (AD) converter discretizes the signal in time and amplitude, assigning digital values to defined time points, ensuring a sufficiently high sampling frequency and fine digitization to accurately represent the original signal in the digital domain.

1.2.2 EMG-Setting data

The EMG machine setting is one of the important parts for acquiring data. It should be adjusted to the same setting as those when control data were collected by the laboratory. Adjusting gain and sweep speed is crucial for displaying waveforms on the screen effectively, avoiding overlap, and an adequate size for proper viewing and measurement. The gain, and to a lesser degree sweep speed, can affect the latency measurement of action potentials, including distal motor latency, duration of compound muscle action potential or Motor unit potential (MUP). Higher gain (increased sensitivity) reveals an earlier onset latency and an increased duration compared to low gain. So, when measuring the latency, the gain and sweep speed should be adjusted to the same special setting as used when recording normal control values. All modern commercially available EMG machines have the functions of temporary storage, and trigger and delay lines. The latter allows the isolation of a single action potential from other action potentials and so enables analysis and confirmation of the consistency of the shape. By delaying each action potential after it has triggered the sweep, it appears in the same position on the screen every time there is a discharge of that unit. This requires an electronic delay circuit and the temporary storing of the recorded MUP. The

sweep is triggered by the potential in real time, but the display is delayed by the preset interval. With this arrangement, the potential studied can occur repetitively and in its entirety in the same spot on the screen for precise measurement of action potential parameters in a short time. Use of a delay line is essential for the analysis of spontaneous activities, of MUPs in the concentric needle EMG and of jitter in single fibre EMG.

1.2.3 EMG-Standard recording

Standard electrophysiological recordings require the use of a minimum of two electrodes since all such recordings are differential, meaning that the signal measured at the first is compared to that obtained at the second. In so-called "unipolar" or "referential" recordings, one electrode is near the active fibres or fibres of interest (the active electrode (E1)) and the second is placed at a distance in a region expected to receive minimal contribution from the active fibres (the reference electrode (E2)). In so-called "bipolar" recordings, the two electrodes are placed in relatively proximity to the active fibres. Whereas unipolar/referential recordings assume that the recording area is electrically silent, in some situations, most notably when recording certain surface motor responses (e.g., ulnar or tibial motor responses), this reference electrode also senses substantial volume-conducted electrical activity. A third "common reference" electrode is also generally employed. Electrical impedance methods typically require a minimum of four electrodes to reduce electrode contact impedance, two for applying an external electrical current through the tissue and two other electrodes for measuring the resulting voltage. Since the electrical current applied is high frequency (e.g., 50 kHz), it does not ex-

cite tissues, there are no bioelectrical signals being generated, and so the electrodes are not referred as "active" or "reference" electrodes, rather both current and voltage electrodes assess the region of tissue beneath and between them. Surface electrodes are used as stimulating or recording electrodes for nervous central system(NCS), for recording surface EMG data, for serving as reference electrodes for monopolar needle EMG, and as a common reference or "ground" electrode. In the past, surface electrodes generally consisted of small round or square reusable metal disks or metallic wire loops (the last for use in measuring sensory potentials from the digits), all employed in conjunction with a conductive electrode gel. However, to reduce the risk of infection and for reasons of convenience, this approach has been increasingly replaced with the use of self-adhesive, disposable electrodes.

Figure 1.3: Self Adhesive Electrodes.

These are generally silver-silver chloride electrodes, with an adhesive conductive gel overlying the electrode surface; they can often be used several times on a single patient before they need to be replaced, generally because the adhesive loses its efficacy. Reusable, saline-saturated Velcro fabric band electrodes are also used to record sensory potentials from the digits. For surface recordings of electrical impedance myography, both reusable metal and disposable carbon-based electrodes have been used. The goal of the recording system is the exact reproduction of the physiological signals generated in muscle cells and peripheral nerves, but artefacts are unavoidable. The most frequent cause of artefact is the electromagnetic radiation from power sources of 50 or 60 Hz, since its frequency is within the physiological range of the EMG signal. However, the neurophysiologist should know other possible causes. These artefacts can have 2 types of origin:

- Technical origin
  - cable motion artefact, with possible additional triboelectric (electrostatic) effect (low frequency range, 1–10 Hz).
  - Transducer noise from displacements in the gel-skin interface, including changes associated with skin stretch.
  - High electrode skin-electrode impedance.
  - Intrinsic noise from the EMG machine (e.g. from amplifiers semiconductors).
  - Biomedical devices (e.g. pacemaker)
- Biological origin

- ECG
- Neighbouring muscles (crosstalk)

It is important to consider several procedures to reduce the impact of artefact on the quality of the recording:

- Isolate electrical circuit of the EMG machine from the ones for other electrical devices, unplug and disconnect unnecessary electrical devices and lights located in the room, avoid use of fluorescent lights and dimmer switches (they give high frequency noise spikes).

- For conduction studies and surface EMG, skin surface should be cleaned using sandpaper, abrasive gel or 70 % alcohol to reduce skin impedance by removing electrically non-conducting elements forming a high-impedance transcutaneous potential generator, which is increased by stretch-deformation.

- Select the appropriate electrode size and their distance according to the muscle volume to reduce the chance of cross-talk. It should be considered that smaller surface electrodes have higher impedance, requiring more careful skin preparation. Double differential recording can be used to eliminate cross-talk in demanding protocols, in the latter technique signals arriving simultaneously at both electrodes are deleted, since propagating signals are time-delayed.

- Filtering the signal to remove frequencies outside the known physiological source is important (like mechanical and electrical noise). However, elimination is not complete for the frequencies above and below the setting limits. Filtering is not useful for cross-talk, since desired and cross

talk signals have similar frequency ranges. Proper patient grounding is essential to reduce electromagnetic noise. The patient ground electrode is attached to the amplifier as a reference to differential inputs to improve rejection ratio mode. A large surface ground electrode or felt band ground electrode is recommended, positioned close to the recording electrode (between stimulator and recording electrode in conduction studies), not overlying electrically active surfaces like as muscle, and with a low electrical resistance ($<$ 3–5 kOhms). Sometimes it is advisable to ground the examiner too, in order to reduce power line artefact. Make sure the power outlet used for the electrodiagnostic system (equipment grounding) has good connection to 'earth'. This is also required for safe operation of the instrument.

- Cables should be short, fixed, shielded, and separated from others (in particular recording and stimulator cables).

- Stimulus artefacts depend on its intensity, duration and distance between recording and stimulation sites. They can distort the waveform and interfere with the accurate measurement of latency with short nerve segments. As always, it is recommended that the lowest supramaximal intensity is used.

Ideally, EMG should be performed in a quiet, temperature-controlled room, separated from any source of electrical noise. It should be considered that when the amplitude and/or decay of the stimulus artefact is an issue, attention needs to be paid to the grounding, skin perspiration, the orientation of the stimulating and recording electrodes, the quality of the skin-electrode

interface and the high-pass filter, for instance, are the recording electrodes dry. If attention to these factors does not fix the problem, the amplification may need to be reduced so that the trace remains within the linear range of the amplifier and A/D converter. Removing artefacts may be even more difficult during electrophysiological examinations in intensive care units. To minimise artefacts, all unnecessary plugs should be removed. [Tankisi *et al.*, 2019]

1.3 Ipsilateral Silent Period

The iSP can be studied using a short single-pulse TMS protocol providing stimulation to the hemisphere ipsilateral to an actively contracted muscle to measure the temporary disruption in the EMG signal. ISPs are thought to be a result of transcallosal inhibition via the posterior mid-body of the corpus callosum. TMS can measure also inhibitory processes as interhemispheric inhibition (IHI) which is specifically a measurement of the transcallosal connections and processing between bilateral primary motor cortices (M1s) . Through a paired pulse paradigm: providing double stimulation (one test stimulus preceded by one conditioning stimulus) over both hemispheres to measure the change of corticospinal excitability in the test hemisphere due to the conditioning stimulus applied to the opposite hemisphere. As silent periods measure inhibition of volitional motor activity, rather than inhibition of MEPs (as is the case for paired pulse methods), silent periods are particularly well suited for investigating the inhibitory effects of cortical and corticospinal control of voluntary motor output. ISP could be quantified by:

iSP duration, the duration of the disrupted EMG signal; iSP area, area of the disrupted EMG signal; and normalized iSP, the area normalized to pre-TMS EMG which takes the muscle contraction level into consideration. All these measures provide a measure of suppression of the ipsilateral EMG.

Greater depth, duration, and area are interpreted as greater IHI. Another common iSP measure includes transcallosal conduction time, which quantifies the speed of signal transmission through the posterior corpus callosum. Transcallosal conduction time is typically calculated as the time elapsed from the onset of the contralateral MEP to the onset of the iSP. Reduction of functional TI has been reported in ALS patients, but the electrophysiological findings seem not to be associated with a decrease of fractional anisotropy (FA) in the motor region of the CC. [Hupfeld *et al.*, 2020]

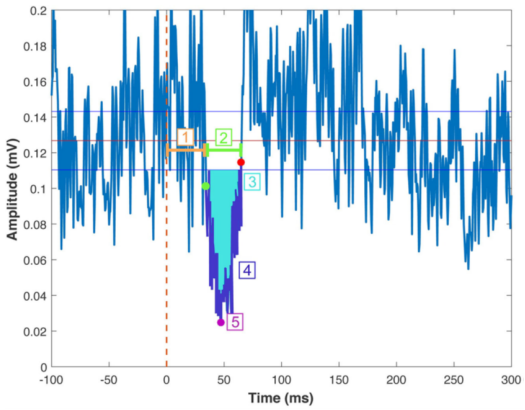

Figure 1.4: An example of average rectified EMG data. The TMS pulse occurred at time = 0 ms. The green and red points indicate the iSP onset and offset, respectively. 1. iSP Latency. 2. iSP Duration. 3. iSP Area. 4. Average iSP Depth. 5. Maximum iSP Depth.

1.4 Functional near infrared spectroscopy

fNIRS is an optical and noninvasive neuroimaging technique that enables the assessment of changes in oxygenated (HbO) and deoxygenated (HbR) hemoglobin concentrations in cortical cortex following neuronal activation. This method involves illuminating the head with near-infrared (NIR) light in the range of $650 - 950$ nm. Taking advantage of the relative transparency of biological tissue within this NIR optical window, the light penetrates through the layers of the scalp, skull, and cerebrospinal fluid to reach the brain tissue.

The complexity of the interaction between NIR light and human tissue arises from the anisotropic and inhomogeneous nature of the tissue across various layers. However, the attenuation of NIR light occurs through absorption and scattering. Absorption involves the conversion of photon energy into internal energy within the medium it travels through, depending on the molecular properties of the material. In human tissue, substances like water, lipids, hemoglobin, melanin, and cytochrome-c-oxidase exhibit different absorbing properties at varying wavelengths. Hemoglobin exists in oxygenated and deoxygenated forms, absorbing NIR light differently. HbO has higher absorption for $\lambda > 800$ nm, while HbR has a higher absorption coefficient for $\lambda < 800$ nm. This difference in absorption is reflected in the color of blood, appearing more red for oxygenated arterial blood and more purple for venous blood. Spectroscopic measurements quantify this color difference. When a specific brain area is active and engaged in a task, the metabolic demand for oxygen and glucose increases, leading to functional hyperemia, an oversupply in regional cerebral blood flow (CBF) to meet the heightened metabolic demand. This results in an increase in HbO and a decrease in HbR

concentrations, detectable through changes in light attenuation measured by fNIRS.

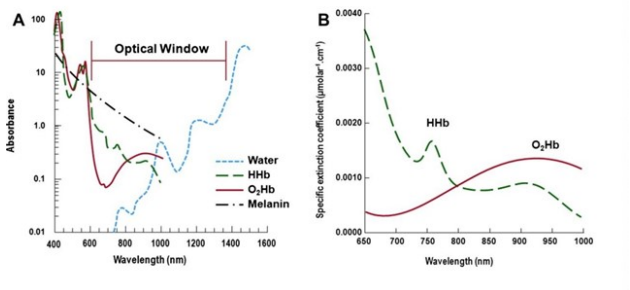

Figure 1.5: Behaviour of HbO and HbR at different wavelengths.

Apart from absorption, NIR light undergoes scattering as it travels through biological tissue. Scattering, occurring much more frequently than absorption, leads to light attenuation. The extent of photon scattering affects the path length, influencing the probability of absorption. Thus, light introduced into the head scatters, diffuses, and penetrates several centimeters through the tissue.

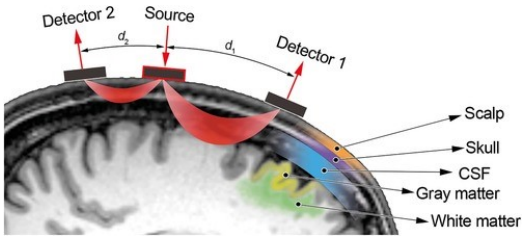

Figure 1.6: Path followed by the NIR photons from the light source to the detector through the different layers of the head.

By placing a light detector at 3,5 cm distance from the NIR light source, backscattered light can be collected, and changes in light attenuation can be measured. As absorption within the NIR optical window is primarily due to HbO and HbR, alterations in light attenuation at a specific wavelength can be expressed as a linear combination of concentration changes in HbO and HbR. Most commercially available systems, commonly referred to as continuous wave (CW) fNIRS instruments, utilize a continuous emission of near-infrared (NIR) light, typically at two or three wavelengths. As illustrated in the figure 1.6, they measure light attenuation (A) resulting from tissue scattering and absorption by estimating the ratio of the injected light (I_{IN}) to the output light (I_{OUT}). By subtracting the initial attenuation measurement from subsequent measurements, changes in attenuation (ΔA) are estimated. These changes are then utilized to derive alterations in the HbO and HbR concentration. This approach assumes that ΔA is only dependent on changes in absorption by the oxygen-dependent hemoglobin chromophores, effectively excluding other factors such as scattering, melanin, and water concentrations, which are unlikely to undergo significant changes during the measurement period. This method is commonly known as the modified Beer–Lambert law (mBLL) or differential spectroscopy and finds widespread application in fNIRS.

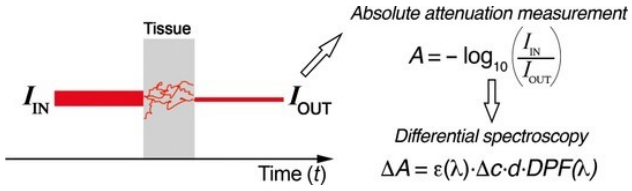

Figure 1.7: Continuous wave devices measure light attenuation due to scattering and absorption based on intensity measurements of the input (I_{IN}) and output (I_{OUT}) light.

CW fNIRS devices can offer information about concentration changes in HbO and HbR but face limitations in resolving absolute baseline concentrations. This limitation arises from their inability to separate and quantify the contributions of absorption and scattering. As a result, measurements of HbO and HbR typically start from zero. Despite this limitation, these systems are well-suited for applications in cognitive neuroscience, where absolute concentrations may not be critical, and functional activity is typically evaluated relative to a baseline. Beyond CW technology-based fNIRS systems, instruments can be categorized into two additional classes: time-domain (TD) and frequency-domain (FD) devices. These alternative classes allow the separation of light absorption and scattering contributions, enabling the determination of absolute HbO and HbR concentrations. FD devices employ intensity-modulated NIR light, while TD systems, more sophisticated in design, incorporate a NIR light source emitting few picosecond pulses and a fast time-resolved detector to recover the time of flight (temporal spread function) of re-emerging photons. The temporal spread function not only provides information on scattered and absorbed light but also on the depth reached by photons within the brain, where longer time spent indicates a

greater distance travelled. The segment of tissue exposed to the NIR light is termed a "channel" and is situated midway between the source and the detector, at a depth approximately half of the source–detector separation. The penetration depth of the light is linked to the source–detector distance,the longer the distance, the deeper the penetration. [Pinti *et al.*, 2020]

Numerous studies have investigated the spatial and depth sensitivity of functional fNIRS on brain tissue, varying the source–detector separations through Monte Carlo simulations. For instance, research proposed that a source–detector separation of 55 mm yields higher sensitivity to adult brain tissue[Strangman *et al.*, 2013]. However, extending the source–detector separation to reach deeper structures compromises the signal-to-noise ratio (SNR) due to increased light absorption probability, resulting in reduced light received by the detector. Therefore, the source–detector separation must strike a balance between depth sensitivity and SNR. Commonly accepted values for this compromise are source–detector separations of 30–35 mm for adult studies and 20–25 mm for studies involving infants. fNIRS measurements are highly sensitive to scalp and skull tissues The presence of noise in fNIRS data is often attributed to systemic activities, which can generate signal changes that mimic or mask true task-evoked hemodynamic responses. Some of these artifacts can be effectively removed by filtering techniques. However, removing other systemic signals can be more challenging and may necessitate more sophisticated signal processing methods. To separate cerebral from systemic activity short-separation channel(SS) has adopted, which are fNIRS channels placed closer to the source-detector pair compared to typical channels. By utilizing the signals from these SS, it is possible to estimate and regress out

systemic activity from the measured signals, thus isolating cerebral hemodynamic responses more accurately.[Wyser *et al.*, 2020]

In general, fNIRS technology can be employed in two configurations based on the number of channels and their arrangement. In its simple, prevalent commercial form, fNIRS utilizes unique distributions of source and detector optical fibers (or optodes) at various locations on the head, each with fixed source–detector separations. Each separation represents a measuring channel, offering a topographical depiction of changes in the concentration of HbO and HbR across the cortical surface. An alternative configuration involves the use of overlapping channels, employing multiple source–detector distances over the head to obtain a tomographical representation of changes in HbO and HbR concentrations across the cortical surface. This latter configuration is known as diffuse optical tomography (DOT), employing denser arrays of channels that sample overlapping brain volumes.

1.4.1 fNIRS vs fMRI

fNIRS provides a cost-efficient and portable alternative to functional magnetic resonance imaging (fMRI) for assessing cortical activity changes based on hemodynamic signals. The fMRI relies on the BOLD(blood-oxygen-level-dependent) contrast. The source of the BOLD contrast is derived from the difference in magnetic susceptibility of deoxygenated blood, which is paramagnetic and oxygenated blood, which is diamagnetic. The fMRI is non-invasive, repeatable, widely available and has superior spatial resolution compared to fNIRS and other neuroimaging techniques. Furthermore, the high-resolution activation maps produced by fMRI allow for visually commu-

nicable results. However the recent technological advancements in modern fNIRS systems have resulted in devices that are increasingly miniaturized, wireless and battery-operated. This has allowed for advancements in the study of neurocognitive processes in unconstrained environments, including studies outdoors and in various other ambulatory settings. To this end, one of the most notable advantages of fNIRS as a neuroimaging tool is the lack of strict restrictions on motion. This stands in stark contrast to fMRI, where complete stillness is required during the acquisition in order to ensure proper data quality and the absence of motion artifacts. Moreover, portable fNIRS devices also allow for paradigms that would be impossible with fMRI, such as investigating the neural correlates of walking and can also be employed to more closely parallel the conditions under which a clinical neuropsychological assessment would actually take place. Furthermore, as functional neuroimaging becomes an increasingly important component of clinical research, the insensitivity of fNIRS to common electrical or magnetic devices, such as hearing aids, pacemakers, or cochlear implants, also serves as a significant advantage where fMRI is limited. However fNIRS has spatial constraints: the signal recording reaches only cortical levels, and the areas to be investigated must be decided in advance. In fact, unlike fMRI, which is capable of whole brain measurement, the number of sources and detectors in the fNIRS setup determines the size of the brain area that can be measured. Similar restrictions on measurement also apply to brain depth: while fMRI is capable of detecting activity in deep cortical and subcortical regions, fNIRS is only able to detect NIR light that penetrates the first few centimeters of cortical tissue, making this one of fNIRS' key limitations. [Scarapicchia *et al.*, 2017]

	fMRI	fNIRS
Strengths	• Non-invasive • Repeatable • Widely available • Superior spatial resolution • Whole brain measurement (lateral surface and depth)	• Non-invasive • Repeatable • Comparable temporal resolution to fMRI • Inexpensive • Portable • Less restriction on motion
Limitations	• Expensive • Strict restrictions of motion • Need for supine position • Noisy scanner • Physiological noise • Restrictions based on metal in the body • Restrictions based on claustrophobia	• Limited to frontal regions and surface analysis • Physiological noise (including superficial scalp signals) • Lacks anatomical information • Interpretation challenges related to multiple sources of vascular signal

Figure 1.8: An overview of strengths and limitations associated with fMRI and fNIRS.

1.4.2 fNIRS Data Analysis

fNIRS is based on principles of optical spectroscopy and the theory of neurovascular coupling. An increase in neuronal activity leads to an elevation in oxygen metabolism, necessary to meet the increased energy demands. Neuronal activation results in changes in cerebral hemodynamics as blood flow is directed towards active brain regions (neurovascular coupling) to supply them with oxygen. These hemodynamic changes lead to an increase in the HbO concentration and a decrease in the HbR concentration in these brain areas, as oxygen supply exceeds the amount consumed locally. These hemoglobin concentration changes are calculated using the mBLL, and then generally followed by the estimation of hemodynamic response function (HRF) by simple block averaging, convolution, or linear estimation models.

Generally during a stimulus event, the hemodynamic response reaches a peak at $\sim$ 5 s after the stimulus onset and goes back to its baseline with a certain delay ($\sim$ 16 s from the stimulus onset). [Yücel *et al.*, 2021] However the response dynamics (e.g., peak and undershoot latency, duration) can vary across different brain regions, task types and design, and participants' age. Leveraging the similarities between hemodynamic signals in fNIRS and fMRI, sophisticated analysis techniques such as statistical parametric mapping based on the General Linear Model (GLM) have been extended to fNIRS data analysis. This approach considers the entire fNIRS time series, utilizing the higher sampling rate (commonly up to 10 Hz) of fNIRS recordings, and provides increased statistical power compared to averaging The GLM represents measured data as a linear combination of functionally distinct components. While block averaging avoids a priori

assumptions about the shape of the HRF, the GLM allows modeling different confounding factors in the fNIRS signal along with the hemodynamic response to the stimulus. The GLM enables simultaneous estimation of the contribution of the fNIRS components and thus provides a less biased estimate of the HRF. GLM regressors' weights at each channel are typically estimated using least squares, minimizing the sum of squared differences between actual and fitted values. Ordinary least squares assumes uncorrelated errors between observations, and hypothesis testing is performed by assessing whether estimated coefficients significantly differ from zero, rejection of the null hypothesis indicates that there is a response to the stimulus.. Single contrasts are tested using t-statistics, while F-statistics test multiple contrasts simultaneously. Second-level GLM analysis estimates population effects using fixed-effects, random-effects, or mixed-effects models. Random-effects models consider both within-subject and between-subject variability, enabling inferences about the population,from which the sample is drawn. Channel-specific effects' statistical significance is assessed by thresholding a test statistic (e.g., t- or F-statistic) at a height z. Multichannel fNIRS systems pose a high risk of type I error due to multiple concurrent statistical tests per channel, necessitating type I error control. For single-channel analyses, statistical inference can rely on uncorrected p-values based on a priori knowledge. However, when analyzing multiple channels, regions, or network components, correcting for multiple comparisons is essential. Multiple comparison correction methods include Bonferroni, Holm, false discovery rate control, effective multiplicity correction, random field theory, or permutation tests. Random field theory suits interpolated fNIRS topographic maps, and

when employing cluster-based inference, the cluster size threshold should be reported with an adjusted p-value.[Yücel *et al.*, 2021]

Data-driven approaches, such as independent component analysis (ICA), principal component analysis (PCA), and task-related component analysis, detect functional activity by separating task-evoked and task-independent components within recorded fNIRS data. Recently, multivariate techniques like multivoxel pattern analysis (MVPA) borrowed from fMRI have been employed to discriminate task-evoked brain activity between experimental conditions. Freeware analysis toolboxes have been developed and listed on the Society for fNIRS to facilitate the application of these analysis methods.

Chapter 2

Materials and Method

2.1 Participants

Fifteen healthy young adults were recruited for this study (age: 26 $\pm$ 6.1, 11 females). All the participants were naive to the purpose of the experiment. They reported no previous history of neurological disorders or orthopedic problems for the right-dominant hand, as determined by the Edinburgh Handedness Inventory [Oldfield, 1971]. Subjects had no contraindication to TMS. The study was conducted in accordance with the 2013 revision of the Declaration of Helsinki on human experimentation. Subjects participated in this study after giving their informed consent.

2.2 Experimental protocol

During the entire experiment three different devices were used: the TMS to stimulate the left hemisphere; the fNIRS, to record the cortical activity

on the right hemisphere; and the EMG, to depict the muscles activity of both hands. The fNIRS montage was performed at the beginning of the experiment. Optodes covered several areas of the right hemisphere and only the prefrontal area of the left hemisphere. Before starting the experiment, the fNIRS signal quality was checked via Aurora software (see section 2.3.2). Then, silver disc surface electrodes were taped to the belly and tendon of the first dorsal interosseous(FDI) muscle to record the motor evoked potentials or muscle contraction from both the right and left FDI muscles. The ground electrode was placed at the wrist. Finally, the TMS was performed with a figure-of-eight coil with wing diameters of 70 mm. The coil was placed tangentially to the left scalp with the handle pointing backward and laterally at a 45° angle to the sagittal plane inducing a postero-anterior current in the brain. The optimal position for the activation of the right FDI muscle was determined by moving the coil in 0.5 cm steps around the presumed hand motor area. Then, TMS intensity was set at 120% of the individual average resting motor threshold.

The average setup time of fNIRS, TMS and EMG was around 45 min, then the experimental procedure began, and it lasted around 30 minutes.

The main experiment consists in three experimental conditions separated by three minutes and presented in a randomized order, (see fig 2.1):

- TMS-uni, where the participant was asked to contract the left hand and the left motor cortex was stimulated by TMS;
- TMS-bil, where the participant was asked to contract both hands and the left motor cortex was stimulated by TMS;

- NoTMS-uni, where the participant was asked to contract the left hand and the TMS was not applied.

In all conditions, the activity of the right hemisphere was recorded through fNIRS. For each condition were presented 25 trials, for a total of 75 trials. Each trial was composed by task and rest , lasting about 22 seconds (see fig. 2.1).

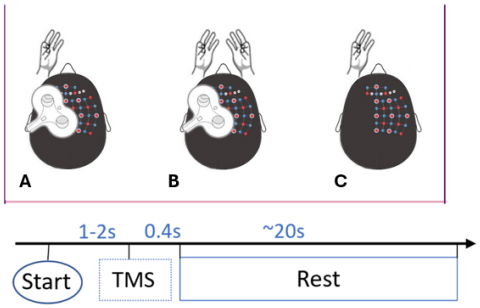

Figure 2.1: Example to explain the experimental paradigm. In A there is the TMS-uni condition, in B the TMS-bi condition and in C the condition without TMS. Start indicates the beginning of the contraction which stops 0.4 sec after the release of the stimulation and the rest begins. When TMS is not present, however there is a contraction of the same duration as the others and then the rest.

2.3 Set_ up

EMG signals were digitalized, amplified, and filtered (20 Hz to 1 kHz) with a 1902 isolated pre-amplifier controlled by the Power 1,401 acquisition interface (Cambridge Electronic Design Limited, Cambridge, UK), and stored on a

personal computer via Signal software (see section 2.3.1) for display and later offline data analysis. The Signal software was also connected to the TMS device and allowed the synchronization of the two devices.

fNIRS data were acquired with a continuous-wave, portable, multichannel NIRS system (NIRSport 2, NIRx Medical Technologies, Berlin, Germany), consisting of 16 LED illumination sources and 16 active detection sensors operating at two continuous wavelengths of near-infrared light (760 nm and 850 nm) to detect changes in concentration of oxy- (HbO) and deoxy- (HbR) hemoglobin. Optodes were arranged on a soft black tissue cap (EasyCap, Germany) on the participants' heads to cover prefrontal, premotor, motor, sensory and parietal brain areas of the right hemisphere. The array was composed of 49 standard channels (3 cm) and 8 short-separation (SS) channels (8 mm). The sampling frequency was set at 11.2 Hz. The LED lighting system is connected via WiFi to a computer, where the Aurora software (see section 2.3.2) allows the fNIRS signal acquisition and visualization.

Figure 2.2: fNIRS components

2.3.1 Signal

Signal is a comprehensive data acquisition and analysis software package that offers a wide range of functionalities. It can be used for simple tasks like acting as a storage oscilloscope, as well as for more complex applications requiring stimulus generation, data capture, control of external equipment, and custom analysis. This versatility makes it suitable for various applications including transient capture, patch and voltage clamp experiments, long-term potentiation (LTP) studies, evoked response experiments, and TMS. In the latter case, fixed, random and pseudo-random pulse sets are output with online and offline waveform averages and measurements of latencies, amplitudes and areas. It, also, can control adjusting stimulator amplitude and timing with checks on stimulator condition during data acquisition. Settings are stored with the corresponding data frame. Signal can also record single and multiple channels of EMG with software control of amplifiers and perform rectification and smoothing at the touch of a button or under script control.

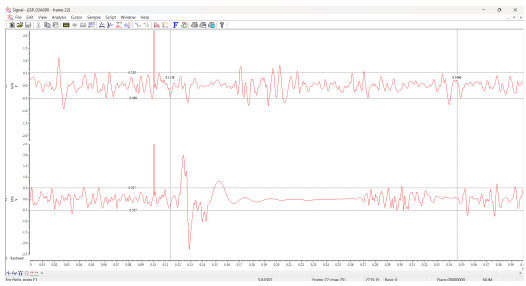

Figure 2.3: Signal interface, with subject record.

Setting up Signal for data capture and analysis is straightforward, and it provides robust sampling and analysis features. The software includes a

built-in script language that automates repetitive tasks and offers additional tools for custom analyses and applications. It also offers suitable functions for specific application areas such as dynamic clamp, whole-cell and patch clamp electrophysiology, evoked response studies, and control of magnetic and other stimulus devices.

Signal can perform Resting Motor Threshold (RMT) measurements using the MTAT 2.0 (PEST) algorithm. Additionally, it has the capability to import data recorded by many other systems, making it a highly versatile system that can analyze existing data.

Optional windows within Signal can display dynamic information in text and images at a large scale. The software also boasts powerful data capture and time-saving analysis functions. Key features of Signal include:

- Recording sweeps of waveform and marker data, either free-running or time-locked to a stimulus or response.
- Performing both online and offline analysis including waveform averaging (with error bars), power spectra, and amplitude histograms.
- Detecting and measuring waveform features in raw data and generating measurements both online and offline in XY views or channels in the data file.
- Marking detected features and events, either interactively, through automated measurement processes, or via a script.
- Generating simple and complex protocols of waveform and digital output and modifying the output interactively even while sampling.

- Automatically triggering script execution at defined times before, during, or after a sampled sweep. Scripts can be used to take measurements, report results, and update further outputs.

In addition, Signal allows users to derive 'virtual channels' defined by user-supplied expressions for channel arithmetic, spectral analysis, and stimulus waveform generation. It offers easy data manipulation using menu or keyboard-driven functions, options for automation and customization of analysis and repetitive tasks, digital filtering (FIR and IIR) via interactive dialogs or scripts, and configuration of multiple views of the same data file with overlay capabilities from multiple sweeps and channels, even during sampling.

Finally, Signal allows for the import of data files recorded with other acquisition systems in various formats including Axon, EDF, HEKA, ASCII, and binary. Users can also export data to other applications as text, binary, or image files, and write .mat files to export data to MATLAB. The Signal data format (CFS) is freely available to programmers wishing to read and write Signal data files. [https://ced.co.uk/products/sigovap, CED]

2.3.2 Aurora

Aurora fNIRS is an intuitive, flexible, and user-friendly software designed to interface with NIRS instruments for signal visualization. With its automated signal optimization algorithm, Aurora fNIRS ensures optimal signal quality before the start of a measurement. Real-time visualization of raw data and HbO and HbR concentration changes is possible in various display modes, including whole-head visualizations. Recorded data can be exported via the integrated Lab Streaming Layer (LSL) protocol, enabling real-time process-

ing in Brain-Computer Interface (BCI) and Neurofeedback paradigms. LSL also allows to received external triggers to identify temporal frame as markers for specific conditions. The navigation pane of Aurora fNIRS 2021.4 is structured into two main sections:

- Main Navigation Pane: Guides the user through the main steps of the recording session sequentially.
- Supporting Navigation Pane: Guides the user through different options or sub-steps for each step of the recording session.

The main steps of a recording session in the main navigation pane are as follows:

- **Setup**: it allows the selection of the measurement device and of the measurement configuration (i.e, the montage).

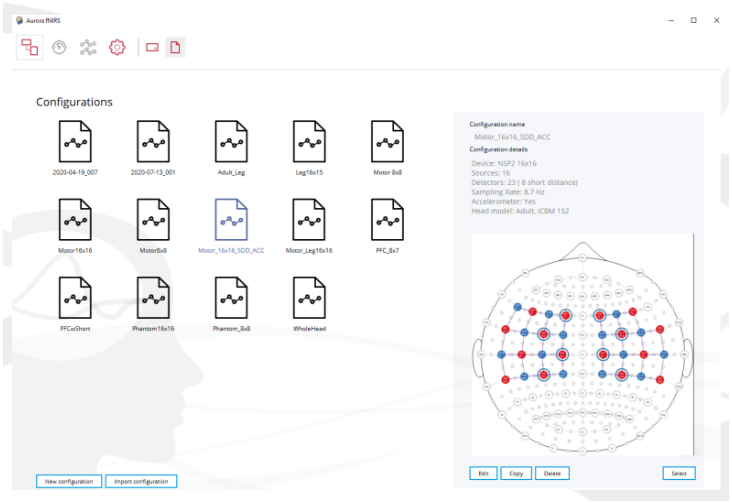

Figure 2.4: Selection of fNIRS montage

- **fNIRS signal Optimization**: before initiating a measurement, Aurora fNIRS performs a signal optimization routine to identify the optimal source brightness and provide feedback on the quality of each channel in the probe layout. The Signal Optimization routine consists of several steps to determine the optimal source brightness for each channel, taking approximately 30 seconds for a 16×16 montage. It is recommended that the subject remains still during this process.

  Metrics such as signal level, dark noise, source brightness, and Coefficient of Variation (CV) are reported for each channel/optode. It is crucial to achieve good signal quality on all channels before proceeding with the recording. Poor signal quality may result from factors such as poor optode-skin contact, presence of hair, improper cable placement, or an incorrect source-detector arrangement. Dark noise measure characterizes a detector's sensitivity, with high levels indicating ambient light interference and the need for action to reduce dark noise. Source brightness level indicates the intensity level required for optimal data quality, adjusted based on factors such as skin-optode contact, hair density, and skin color. If short-distance measures are set up, the short-distance detectors are displayed as rings around their respective sources, providing signal amplitudes and dark noise values similar to standard detectors. [https://nirx.net/software, Nirsitea]

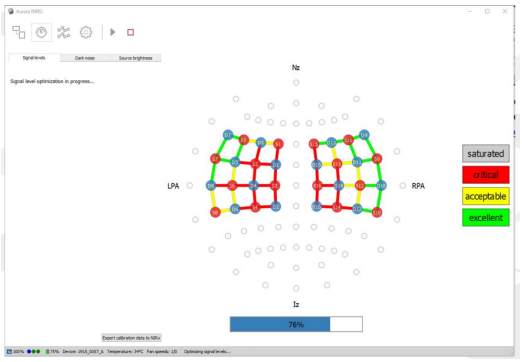

Figure 2.5: NIRS editing calibration, where the green channels meaning a good quality signal and red meaning bad quality signal.

- **Record**: this step lets to start and stop the recording.

2.4 fNIRS_ montage

Despite fNIRS having several advantages such as silence, portability, and robustness to motion, one of its limitations is the inability to study all areas simultaneously. Therefore, it is necessary to make a priori choices regarding the areas to be investigated. The NIRSite software is an open-source application which allows the setting of the montage to load on Aurora interface.

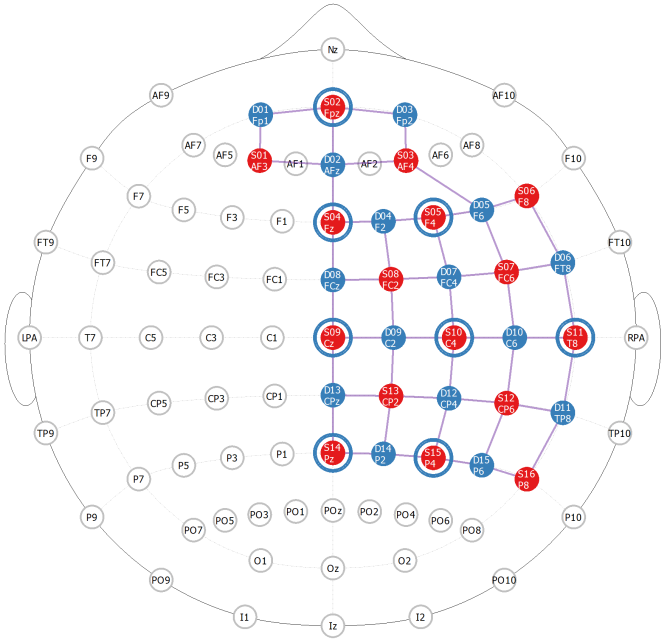

Figure 2.6: fNIRS_ montage

2.4.1 Nirsite

The NIRSite 2021.4 program is designed to offer a user-friendly approach to specifying the arrangement of NIRS sources and detectors, also known as a montage, which can be readily used with NIRStar and Aurora fNIRS systems. NIRSite utilizes MNI head models, derived from MRI scans, and provides options to either manually position sources and detectors on the scalp, with EEG landmarks as reference points, or import digitized coordinates of the optodes. The latest version of NIRSite, 2021.4, includes various enhancements such as different infant head models and the automatic creation of short-distance channels. Some of the actions that can be performed

with nirsite[https://nirx.net/software, Nirsiteb] are:

- Effortless addition of short-distance channels;
- Manual manipulation of measurement channels;
- Renaming source and detector labels;
- Creation of montages in the two-dimensional view;
- Automatic export to NIRStar and Aurora montage folders.

2.4.2 BA_ association

NIRS records signals from each channel (source-detector pair) therefore an association between these channels and the areas of the cortex is necessary to be able to interpret the data. To determine in an automatic way which area was associated to each channel, a custom-made MATLAB script was developed. The first step was to associate to each channel the relative source and detector. Then, for each source and detector a label corresponding to the position on the cap in the EEG 10-10 system was assigned. In the second step, through fOLD software [Morais *et al.*, 2018], all possible label pairings defining the various possible BA were considered. This allows to associate to each label pairing the BA with the highest probability. The last step was to extract the BA for each of the 57 channels by comparing the label pairing obtained by the two previous steps.

2.5 Analysis

The analysis phase begins by conducting separate analyses on TMS-EMG data and fNIRS data. Subsequently, a correlation is performed between the outputs of these analyses.

2.5.1 iSP

As regards the analysis of iSP data, the iSP values were evaluated in the trace, considering at least 20 trial per condition of the 25 recorded. These parametres were obtained by averaging the rectified EMG traces recorded from the left hand for both TMS-uni and TMS-bil conditins. In NoTMS condition, as there was no stimulation, no ISP was computed.

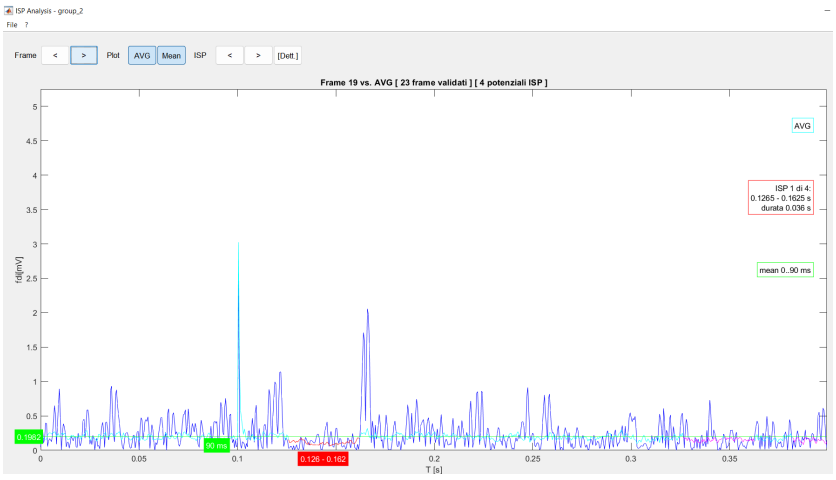

Figure 2.7: ISP analysis

The iSP was evaluated by considering: the onset of the iSP, defined as the point after cortical stimulation at which EMG activity became consistently below the mean amplitude of EMG activity preceding the cortical stimulus; the duration of the iSP, calculated by subtracting the start time from the end time (i.e., the first point after the start of the iSP at which the EMG activity level returned to the average EMG signal); and the normalized iSP area, calculated using the following formula:

$$\frac{[(EMG\ mean\ x\ iSP\ duration\ ) - (area\ under\ the\ iSP\ )]}{EMG\ signal\ preceding\ the\ cortical\ stimulus} \tag{2.1}$$

The normalized iSP area is a stable measurement and is independent of the level of contraction in the ipsilateral muscles.[Bortoletto *et al.*, 2021]

2.5.2 fNIRS

fNIRS data pre-processing was performed in MATLAB utilizing Homer3 functions. Homer3 is an open-source MATLAB toolbox for analysis of fNIRS data and for creating maps of brain activation. The first step was to remove noisy channels from analysis and then converting the intensity of remaining channels to Optical Density(OD). Motion artifacts were identified as the segment of data around time points that exhibited a signal change greater than almost one of two imposed thresholds. One threshold was the standard deviation threshold which was computed as 12 times the standard deviation of the entire channel signal, the other was the amplitude threshold and was set to 0.5 OD.[Iester *et al.*, 2023] Then, motion artifacts were corrected by

applying a combination [Lorenzo *et al.*, 2013] of spline (p = 0.99) [Scholkmann *et al.*, 2010] and wavelet (iqr=0.5) [Molavi and Dumont, 2010] motion correction techniques. Then, the identification of motion artifacts was repeated to detect residual motion artifacts. A band-pass filter (0.01–3 Hz) was applied to remove slow drifts, and high frequencies components. Then, trials falling within the time points identified as residual motion artifacts were discarded from hemodynamic response function (HRF) calculation. An age-dependent differential pathlength factor was computed for each participant [Scholkmann *et al.*, 2013], and then the HbO concentration changes were computed through the modified Beer-Lambert law [Delpy *et al.*, 1988]. To calculate the mean HRF for each block, participant, and channel, a General Linear Model (GLM) was applied. Iterative weighted least squares were used to solve the GLM [Brundin *et al.*, 2013]. A set of a consecutive sequence of gaussian functions with a spacing and standard deviation of 2 s was used as temporal basis functions for HRF.

Then, concentration change signals of channels belonging to the same BA were averaged obtaining 18 regions of interest. This whole procedure was done for each of the 3 conditions. The block average interval for stimulus onset was set from -2 to 23 s. To remove the physiological noise an additional regressor in the GLM was added. For each standard channel, the most correlated SS channel was used as regressor. For each participant, condition, and BA, the average of the HbO mean hemodynamic responses in the range between 1 and 7 s after stimulus onset was computed and chosen as a metric for statistical analyses. Active BAs were selected by performing a two-tailed t-tests to detect changes in HbO concentration during the task

compared to zero. Active areas had to survive multiple comparisons correction (FDR). Statistical analysis was performed on the BA found to be active in at least one condition. To compare the three different conditions, concentration changes were analyzed by means of repeated measures ANOVA with COND (3 levels: TMS-uni, TMS-bil, NoTMS), and BA (20 levels: active BAs) as within-subject factor. Post-hoc analysis was performed using Fisher's Least Significant Difference (LSD) test.

2.5.3 Correlation

In both TMS-uni and TMS-bil, the Pearson correlation betweenthe ISP area and the HbO concentration changes was performed. All active BAs were correlated with ISP area. Then areas which were statistically correlated with the iSP area were used as predictor variables in a stepwise regression model. Stepwise regression is the step-by-step iterative construction of a regres- sion model that involves the selection of independent variables to be used in a final model. It involves adding or removing potential explanatory variables in succession and testing for statistical significance after each iteration. The goal of stepwise regression is to build a regression model that includes all of the predictor variables that are statistically significantly related to the response variable. There are 2 main approaches to step wise regression:

- Forward-selection,starts with no explanatory variables and then adds variables, one by one;
- Backward-elimination starts with all possible explanatory variables and then discards the least statistically significant variables, one by one.

In this study, a forward-selection approach was used.

Chapter 3

Results

3.1 BA_ association

Regarding the association of Brodmann areas with the channels, the outcome is illustrated in the figure 3.1. Each area is linked with one or more channels along with their respective characteristics. The areas that were associated with the channels of the montage performed for the experiment of this thesis work are: BA10, BA9, BA45, BA46, BA44, BA48, BA43, BA2, BA21, BA22, BA5, BA37, BA8, BA7, BA6, BA4, BA38, BA39, and BA40.

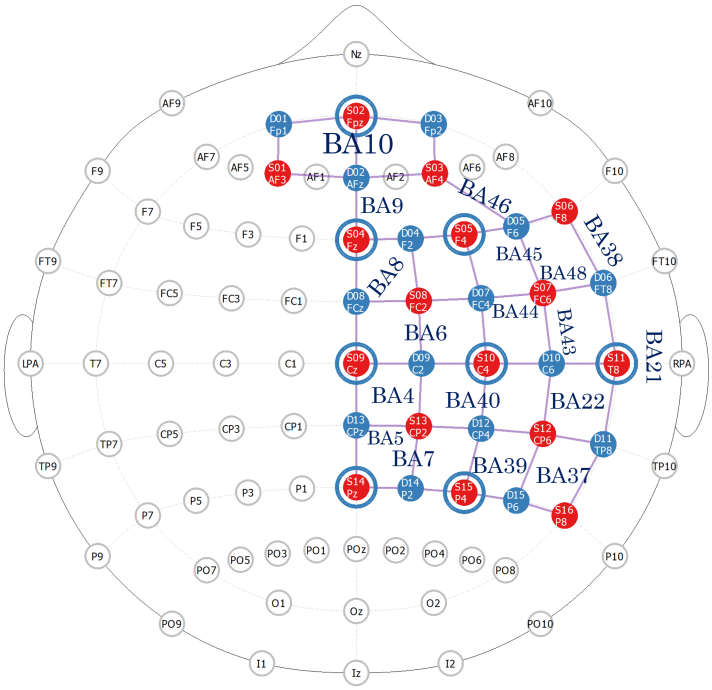

Figure 3.1: Association between channels and BA

3.2 fNIRS_ data

From the analysis of hemodynamic responses, eighteen BAs out of twenty were found to be active. In all the conditions, a general increasing of HbO concentration changes was found in sensotimotor areas and also in associative and parietal areas. In both TMS conditions, HbO concentration changes seem to reduce in several areas.

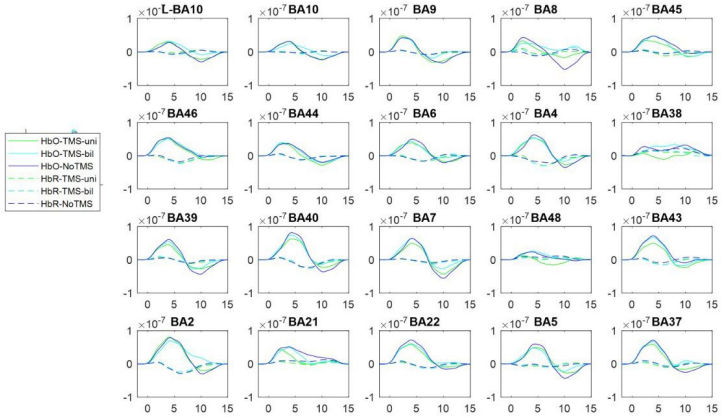

Figure 3.2: Hemodinamic response.

3.3 Correlation between iSP_ data and fNIRS_ data

In the TMS-uni condition, the correlation analysis revealed a significant correlation between the ISP area and BA4, BA5, and BA40 HbO concentration changes (p=0.011, p=0.007 and p=0.024 ,respectively) (see Figure 3.3). In

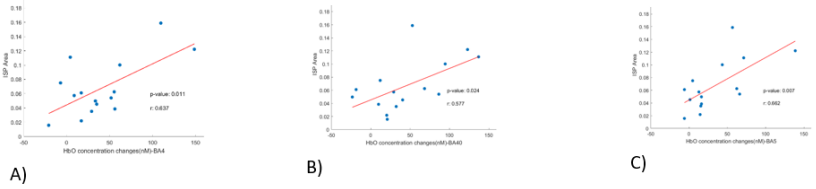

Figure 3.3: Three BAs were found to be statistically correlate with the iSP in TMS-uni condition. A) BA4, B) BA5, and C) BA40

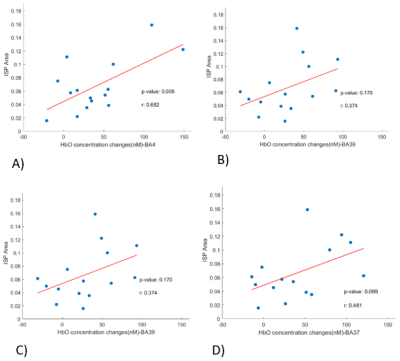

Figure 3.4: Four BAs were found to be statistically correlate with the iSP in TMS-bil condition. A) BA4, B) BA40, C) BA39, D)BA37

the TMS-bil condition, the correlation analysis revealed a significant correlation between the ISP area and BA4, BA39, BA37 and BA40 HbO concentration changes (p=0.025, p=0.041, p=0.030 and p=0.006 ,respectively) (see Figure 3.4).

3.4 Stepwise regression

As regards the analysis done through the stepwise regression, asingle regression model was observed. This model explains the variation in the dependent variable, selecting the best predictive variables. In the figure 3.9 and 3.10 it's possible to note that the p-value of the F- statistics is a very small, highly significant value. Therefore, at least one of the predictor variables is related in a statistically significant manner to the outcome variable. In the TMS-uni condition, BA5 was the only predictor of the model (p=0.007), while in the TMS-bil condition both BA4 and BA40 were predictors of the iSP area (p= 0,04 and p= 0,013, respectively).

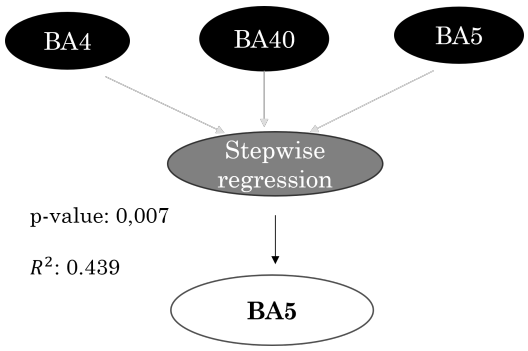

Figure 3.5: Step wise regression in TMS-uni Condition, using only the BA that correlated.

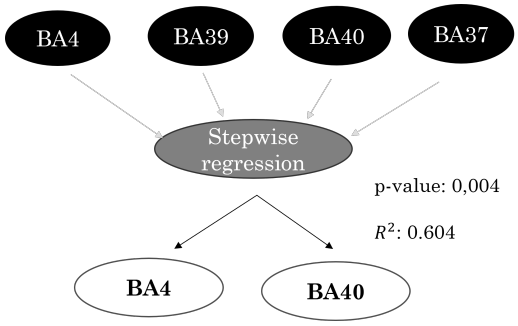

Figure 3.6: Step wise regression in TMS-bil Condition, using only the BA that correlated.

3.5 Discussion

In this work, for the first time, we showed cortical correlates related to the ipsilateral silent period of the contralateral cortex. We simultaneously used TMS, EMG and fNIRS to study the iSP and its neural correlates. From a behavioral point of view, we found a greater inhibition in the TMS-bil condition compared to the TMS-uni condition. These results confirm the literature[Giovannelli1 *et al.*, 2009]. From a neural point of view, the first evidence was to observe the neural correlates during a maximal isometric contraction. An increment in HbO concentration changes was observed not only in the motor cortex, but also in parietal areas. This result suggests that the isometric contraction involves also higher order areas. Then, we studied how the hemodynamic responses could be modulated by the TMS stimulation of the contralateral hemisphere. We observed a decrease in HbO concentration changes that could be explained as an inhibition. Moreover, this decrease is associated with a suppression in the EMG trace. However, performing the correlation between the iSP area and the fNIRS data, we came into a para-

dox: a higher iSP area corresponded to a higher HbO concentration change in BA4. But the higher the iSP area, the higher the inhibition. Thus, it seems that a higher inhibition is related to a higher request of oxygen. To explain this paradox, we can argue that the fNIRS measurement could reveal the activity of either pyramidal neurons or inter-inhibitory neurons. Since we have both an increase in the hemodynamic response and in the iSP area, we hypothesize that the increase in BA4 is due to the activity, and thus the request of oxygen, of the inter-inhibitory neurons. First, the TMS stimulation depolarizes neurons in the left motor cortex, then, the signal goes through the corpus callosum fibers and achieves the right hemisphere. A family of inhibitory interneurons, located in the 3rd layer, was activated and inhibited the corticospinal tract, in the 5th layer. Therefore, the resulting activity is a combination of increased hemodynamic activity of the inhibitory interneurons and a decrease in activity of the pyramidal neurons. This evidence was revealed in both the TMS-uni and TMS-bil conditions. In the TMS-uni condition also in BA40 and BA5 the same trend in correlation was found, while in TMS-bil the same trend was shown in BA40, BA39 and BA37. These results are probably due to the relationship between these areas and BA4. However, further analyses are required to explain the global trend of the signal. Finally, the stepwise regression revealed that the iSP area in the TMS-uni condition was significantly explained by BA5, while in the TMS-bil condition by both BA4 and BA40. The contribution of parietal areas to iSP area could be explained by a feedback mechanism: the motor area sends the inhibitory signal to the periphery, and then the alteration of the peripheral signal (EMG disruption) is received at a parietal level which responds to

indicate that something changed in the periphery. In the TMS-bil condition, the BA4 contribution in stepwise model can be explained by a forward mechanism: activity in BA4 directly explains the ISP area. The reason why the BA4 is present only in the TMS-bil condition is probably due to the higher inhibition compared to the TMS-uni condition.

Chapter 4

Conclusion

In this study, for the first time, we investigated the neural correlates of the ipsilateral silent period. The areas active during maximal isometric contraction are modulated in the presence of the ipsilateral silent period. Specifically, there is a decrease in the HbO concentration changes. Furthermore, the correlation between the ISP area and HbO concentration changes in BA4 suggests that the activity detected by fNIRS may reflect the activity of different populations of neurons, inhibitory interneurons, and pyramidal neurons. These innovative results open up several avenues for future studies and provide an excellent starting point for understanding the dynamics of the ipsilateral silent period, which are still unknown.

Bibliography

[Al-Ayyad *et al.*, 2023] Muhammad Al-Ayyad, Hamza Abu Owida, Roberto De Fazio, Bassam Al-Naami, and Paolo Visconti. Electromyography monitoring systems in rehabilitation: A review of clinical applications, wearable devices and signal acquisition methodologies. *MPDI Journals*, 2023.

[Bortoletto *et al.*, 2021] Marta Bortoletto, Laura Bonzano, Agnese Zazio, Clarissa Ferrari, Ludovico Pedullà, Roberto Gasparotti, Carlo Miniussi, and Marco Bove. Asymmetric transcallosal conduction delay leads to finer bimanual coordination. *Brain Stimulation*, 2021.

[Brundin *et al.*, 2013] Patrik Brundin, Roger A Barker, P Jeffrey Conn, Ted M Dawsonand Karl Kieburtzand Andrew J Lees, Michael A Schwarzschild, Caroline M Tanner, Tom Isaacs, Joy Duffen, and Helen Matthewsand Richard K H Wyse. Linked clinical trials–the development of new clinical learning studies in parkinson's disease using screening of multiple prospective new treatments. *IOS press*, 2013.

[Delpy *et al.*, 1988] D T Delpy, M Cope, P van der Zee, S Arridge, S Wray, and J Wyatt1. Estimation of optical pathlength through tissue from direct

time of flight measurement. *IOP science*, 1988.

[Giovannelli1 *et al.*, 2009] Fabio Giovannelli1, Alessandra Borgheresi, Fabrizio Balestrieri, Maria Pia Viggiano Gaetano Zaccara1, Massimo Cincotta1, and Ulf Ziemann. Modulation of interhemispheric inhibition by volitional motor activity: an ipsilateral silent period study. *Physiol*, 2009.

[https://ced.co.uk/products/sigovap, CED] CED.

[https://nirx.net/software, Nirsitea] Nirsite.

[https://nirx.net/software, Nirsiteb] Nirsite.

[Hupfeld *et al.*, 2020] K.E. Hupfeld, C.W. Swansonand B.W. Fling, and R.D. Seidler. Tms-induced silent periods: A review of methods and call for consistency. *neuroscience method*, 2020.

[Iester *et al.*, 2023] Costanza Iester, Monica Biggio, Simone Cutini, Sabrina Brigadoi, Charalambos Papaxanthis, Giampaolo Brichetto, Marco Bove, and Laura Bonzano. Time-of-day influences resting-state functional cortical connectivity. *frontiers in neuroscience*, 2023.

[Klein *et al.*, 2022] Franziska Klein, Karsten Witt Stefan Debener, and Cornelia Kranczioch. *fMRI-based validation of continuous-wave fNIRS of supplementary motor area activation during motor execution and motor imagery.* Scientifics reports Journal, 2022.

[Klomjai *et al.*, 2015] Wanalee Klomjai, Rose Katz, and Alexandra Lackmy-Vallée. Basic principles of transcranial magnetic stimulation (tms) and repetitive tms (rtms). *Annals of physical and rehabilitation medicine*, 2015.

[Lorenzo *et al.*, 2013] Renata Di Lorenzo, Laura Pirazzoli, Anna Blasi, Chiara Bulgarelli, Yoko Hakuno, Yasuyo Minagawa, and Sabrina Brigadoi. Recommendations for motion correction of infant fnirs data applicable to multiple data sets and acquisition systems. *NeuroImage*, 2013.

[Molavi and Dumont, 2010] Behnam Molavi and Guy A Dumont. Wavelet based motion artifact removal for functional near infrared spectroscopy. 2010.

[Morais *et al.*, 2018] Guilherme Augusto Zimeo Morais, Joana Bisol Balardin, and João Ricardo Sato. fnirs optodes' location decider (fold): a toolbox for probe arrangement guided by brain regions-of-interest. *Scientific Rep*, 2018.

[Oldfield, 1971] R C Oldfield. The assessment and analysis of handedness: the edinburgh inventory. 1971.

[Pinti *et al.*, 2020] Paola Pinti, Ilias Tachtsidis, Antonia Hamilton, Joy Hirsch, Clarisse Aichelburg, Sam Gilbert, and Paul W. Burgess. *The present and future use of functional near-infrared spectroscopy (fNIRS) for cognitive neuroscience.* Annals of the New York Academy of Sciences journals, 2020.

[Rebello-Sanchez *et al.*, 2022] Ingrid Rebello-Sanchez, Joao Parente, Kevin Pacheco-Barrios, Anna Marduy, Danielle Carolina Pimenta, Daniel Lima, Eric Slawka, Alejandra Cardenas-Rojas, Gleysson Rodrigues Rosa, Kamran Nazim, Abhishek Datta, and Felipe Fregni. *Measuring Contralateral*

Silent Period Induced by Single-Pulse Transcranial Magnetic Stimulation to Investigate M1 Corticospinal Inhibition. joVE Journal, 2022.

[Scarapicchia *et al.*, 2017] Vanessa Scarapicchia, Cassandra Brown, Chantel Mayo, and Jodie R. Gawryluk. *Functional Magnetic Resonance Imaging and Functional Near-Infrared Spectroscopy: Insights from Combined Recording Studies*. Frontiers in Human Neuroscience, 2017.

[Scholkmann *et al.*, 2010] F Scholkmann, S Spichtig, T Muehlemann, and M Wolf. How to detect and reduce movement artifacts in near-infrared imaging using moving standard deviation and spline interpolation. *IOP*, 2010.

[Scholkmann *et al.*, 2013] Felix Scholkmann, Martin Wolf, and Ursula Wolf. The effect of inner speech on arterial co2 and cerebral hemodynamics and oxygenation: a functional nirs study. *Springer link*, 2013.

[Smith and Hargrove, 2013] Lauren H. Smith and Levi J. Hargrove. Comparison of surface and intramuscular emg pattern recognition for simultaneous wrist/hand motion classification. *IEEE*, 2013.

[Strangman *et al.*, 2013] Gary E Strangman, Zhi Li, and Quan Zhang. Depth sensitivity and source-detector separations for near infrared spectroscopy based on the colin27 brain template. *Plos one*, 2013.

[Tankisi *et al.*, 2019] Hatice Tankisi, David Burke, Liying Cui, Mamede de Carvalho, Satoshi Kuwabara, Sanjeev D Nandedkar, Seward Rutkove, Erik Stålberg, Michel J A M van Putten, and Anders Fuglsang-Frederiksen. Standards of instrumentation of emg. *Clinical Neurophysiology*, 2019.

[Tofts, 1990] P S Tofts. The distribution of induced currents in magnetic stimulation of the nervous system. *Physics in medicine and biology*, 1990.

[Wyser *et al.*, 2020] Dominik Wyser, Michelle Mattille, Martin Wolf, Olivier Lambercy, Felix Scholkmann, and Roger Gasserta. *Short-channel regression in functional near-infrared spectroscopy is more effective when considering heterogeneous scalp hemodynamics.* Neurophotonics Journal, 2020.

[Yücel *et al.*, 2021] Meryem A. Yücel, Alexander v. Lühmann, Felix Scholkmann, Judit Gervain, Ippeita Dan, Hasan Ayaz, David Boas, Robert J. Cooper, Joseph Culver, Clare E. Elwell, Adam Eggebrecht, Maria A. Franceschini, Christophe Grova, Fumitaka Homae, Frédéric Lesage, Hellmuth Obrig, Ilias Tachtsidis, Sungho Tak, Yunjie Tong, Alessandro Torricelli, Heidrun Wabnitz, and Martin Wolf. *Best practices for fNIRS publications.* Neurophotonics Journal, 2021.

Ringraziamenti

Ringrazio la Prof.ssa Laura Bonzano e il Prof. Marco Bove per la loro disponibilità e per le conoscenze trasmesse in questo percorso. Ringrazio le Dott.sse Costanza Iester e Alice Bellosta per il loro supporto costante, le dritte indispensabili e il loro aiuto nella realizzazione di ogni capitolo della mia tesi.

Il ringraziamento più importante va alla mia famiglia. Su tutti i miei genitori che in questi anni mi hanno sostenuto in tutte le mie scelte con pazienza incoraggiandomi a fare sempre di più, e per avermi aiutato a superare i momenti più difficili. Ai miei fratelli e le mie cognate perchè sempre presenti e pronti a rispondere ad ogni mio "richiamo" d'aiuto, con i loro preziosi consigli. Alla mia nipotina Cloe che ha rallegrato ogni mia giornata.

Ringrazio Simona per essere sempre al mio fianco. Grazie per aver ascoltato i miei sfoghi, grazie per tutti i momenti di spensieratezza.

Grazie anche alle mie colleghe ma soprattuto amiche Robi (la miglior coinquilina di sempre) Adri e Sam che hanno iniziato questo percorso con me e lo hanno reso meraviglioso, e a tutti i colleghi con cui ho trascorso splendidi momenti in questi ultimi 3 anni.

Ringrazio, infine, i miei amici e tutti i miei parenti che mi sono stati sempre vicini in questi anni.